American Mineralogist, Volume 84, pages 299–310, 1999

Thermodynamics and kinetics of cation ordering in $MgAl_2O_4$ spinel up to 1600 °C from in situ neutron diffraction

Simon A.T. Redfern,[1,*] Richard J. Harrison,[2] Hugh St.C. O'Neill,[3] and David R.R. Wood[1]

[1]Department of Earth Sciences, University of Cambridge, Downing Street, Cambridge, CB2 3EQ, U.K.
[2]Institut für Mineralogie, Universität Münster, Corrensstrasse 24, D 48149, Münster, Germany
[3]Research School of Earth Sciences, Australian National University, Canberra, ACT 0200, Australia

Abstract

The temperature dependence of the cation distribution in synthetic spinel ($MgAl_2O_4$) was determined using in-situ time-of-flight neutron powder diffraction. Neutron diffraction patterns of stoichiometric $MgAl_2O_4$ and slightly non-stoichiometric $Mg_{0.99}Al_2O_4$ samples were collected under vacuum on heating from room temperature to 1600 °C, and the cation distribution was determined directly from site occupancies obtained by Rietveld refinement. The equilibrium non-convergent ordering has been analyzed using both the O'Neill-Navrotsky and Landau thermodynamic models, both of which fit the observed behavior well over the temperature range of the measurements. Fitting the data between 560 °C and 1600 °C using the O'Neill and Navrotsky (1983) thermodynamic model yields $\alpha = 32.8 \pm 0.9$ kJ/mol and $\beta = 4.7 \pm 2.0$ kJ/mol. The fit to the Landau expression for ordering gives values of $T_c = 445 \pm 109$ K and $c' = 1.62 \pm 0.21$. This confirms suggestions that the sign of the β coefficient in $FeAl_2O_4$ and $MgAl_2O_4$ is positive, and opposite to that found in other 2–3 oxide spinels. Non-equilibrium order-disorder behavior below 600 °C has been analyzed using the Ginzburg-Landau model, and successfully explains the time-temperature dependent relaxation behavior observed in the inversion parameter. Changing the stoichiometry, even by as little as 1 mol% Mg-deficiency, significantly reduces the degree of order.

Introduction

Temperature-dependent cation disordering of Mg and Al between the octahedrally and tetrahedrally coordinated sites in the spinel ($MgAl_2O_4$) has considerable petrologic importance. High-temperature disorder in spinel could stabilize it with respect to other phases in a mineral assemblage. For example, $MgAl_2O_4$ is the dominant component in the spinel phase of the Earth's shallow mantle, but it reacts at depths of 50–80 km according to the idealized reaction: $MgAl_2O_4 + 2Mg_2Si_2O_6 = Mg_2SiO_4 + Mg_3Al_2Si_3O_{12}$ (i.e., spinel + pyroxene = olivine + garnet). This region spans the depths from which many types of basaltic magma are thought to originate. Determining the exact stability limits of spinel in natural, chemically complex systems is, therefore, necessary to understand the detailed chemistry of basalts. This requires accurate thermochemical data, which are only obtainable if the cation distribution is known (so that the zero-point entropy may be calculated). Preliminary investigations, by Klemme et al. (1997), of the spinel lherzolite to garnet lherzolite transition at high temperatures (1300 to 1500 °C), have revealed a change in the solubility of Al in pyroxenes at these *T*s. Interpretation of this phenomenon depends on understanding the Mg/Al order-disorder in spinel. This may also pertain to the controls on Al_2O_3 in mantle-derived partial melts. Another example of the importance of understanding the high-*T* equilibrium order in spinel is that the Fe_3O_4 component in natural spinels may be used to calculate the redox state at which planetary material is equilibrated. This information is relevant to the processes that lead to the accretion and core formation of the terrestrial planets. Accurate modeling of the activity of Fe_3O_4 in complex Mg-Fe-Al-Cr-O spinels requires knowledge of cation distributions, starting with the simple end-member components including spinel ($MgAl_2O_4$) itself.

The majority of spinels show some degree of disorder, with $MgAl_2O_4$ being close to the "normal" spinel configuration $^{[4]}A^{[6]}B_2O_4$. The alternative ordering scheme $^{[4]}B^{[6]}(AB)O_4$ is termed "inverse." Any intermediate partly disordered state may be expressed as a mix of these two end-members, with a general formula $^{[4]}(A_{1-x}B_x)^{[6]}(B_{2-x}A_x)O_4$, where *x* is the "inversion parameter." The degree of order may, alternatively, be expressed as an order parameter, denoted *Q*, which varies from $Q = 1$ for completely ordered normal spinel to $Q = 0$ for a random arrangement of cations (with, on average, ⅓ of an A atom and ⅔ of a B atom on every crystallographic site), to $Q = -0.5$ in

* E-mail: satr@esc.cam.ac.uk

0003–004X/99/0003–0299$05.00

inverse spinel. The relationship between Q and x is, therefore, $Q = 1 - 3/2x$. The order-disorder process in spinel is termed ''non-convergent,'' because there is no symmetry change upon disordering, and a completely disordered state is approached asymptotically upon increasing temperature.

The wide importance of understanding cation ordering in $MgAl_2O_4$ has led to many experimental studies to elucidate its high-temperature behavior. Certain experimental difficulties are associated with the study of site occupancies in this phase, however. The standard methods of determining cation distributions in spinels [such as X-ray diffraction (XRD), Mössbauer spectroscopy, or magnetic measurements] cannot be applied in a direct manner, so somewhat unusual or indirect methods have been used. These include ESR of impurity Cr cations (Schmocker and Waldner 1976), changes in bond lengths as determined from XRD (Menegazzo et al. 1997), and ^{27}Al MAS-NMR (Brun and Hafner 1962; Gobbi et al. 1985; Wood et al. 1986; Millard et al. 1992). These studies neither agree with one another, nor do they fit the simple thermodynamic description found to be adequate for other spinels. One major problem is reliance on quenching disordered states from high temperatures, and assumptions that the results obtained at ambient temperature accurately reflect the equilibrium state at the annealing temperature. In particular, it is important to demonstrate that the samples have been annealed for sufficient time to reach equilibrium at low temperatures, and conversely for quenched samples, that the quenching has been rapid enough to preserve equilibrium at high temperatures. The kinetics of Mg-Al exchange between the tetrahedral and octahedral sites are sufficiently rapid to prevent quenching of states of disorder for any spinel above 1300 °C or so, which may be regarded as a closure temperature for the anneal and quench method.

Some of the few high-temperature structural studies on spinel suggested that it undergoes a discrete convergent structural phase transition of some sort at temperatures between 600 and 700 °C. Using high-temperature XRD, Yamanaka and Takéuchi (1983) observed changes in the oxygen coordinates and thermal expansion in this temperature range. The dilatometric study of Suzuki and Kumazawa (1980), and the electric conductivity measurements of Weeks and Sonder (1980) also revealed evidence for anomalous changes in the structure at these temperatures. Furthermore, some ambient temperature XRD (Grimes and Thompson 1981) and electron diffraction studies (Hwang et al. 1973; Mishra and Thomas 1977) suggested (on the basis of the presence of $hk0$ reflections with $h + k = 4n + 2$) that the space group of spinel is $F\bar{4}3m$, rather than the conventionally assumed $Fd3m$. Smith (1978) and Tokonami and Horuchi (1980) dismissed these results as effects arising from double diffraction.

Peterson et al. (1991) used in situ, high-temperature, neutron powder diffraction study of synthetic $MgAl_2O_3$ to obtain absolute site occupancies (and hence the degree of long-range order) directly by exploiting the relatively strong (40%) nuclear-scattering contrast between Mg and Al. Their study was, however, limited to temperatures between 600 and 1000 °C, and cannot reliably be extrapolated to the temperatures of petrological interest. Here, we report the results of a new in situ neutron diffraction study of well-characterized $MgAl_2O_4$ between room temperature and 1600 °C. The results from neutron diffraction provide an absolute calibration of earlier work, explain the structural discontinuities observed in earlier studies at intermediate temperatures, and are used to develop a reliable thermodynamic and kinetic model for cation ordering in spinel. It is known that non-stoichiometry and impurity content affects the cation distributions in spinel (Schmoker and Waldner 1967). We investigate the influence of non-stoichiometry on the thermodynamic equilibrium degree of order as a function of temperature by measuring a Mg-deficient sample as well as a stoichiometric sample. Finally, we compare the order-disorder behavior of spinel with that of hercynite ($FeAl_2O_4$).

Experimental methodology

Two samples were synthesized from oxide powders and dried at 1100 °C prior to weighing. The first sample was synthesized from a 14 g stoichiometric mix of MgO (99.999%) and Al_2O_3 (99.99%) oxide powders, weighed out and homogenized by grinding under acetone in an agate mortar. The oxide mix was then pressed into several pellets using a 0.5 inch diameter WC die. The pellets were sintered for a period of 42 h at 1500 °C. The pellets were then quenched by dropping them to the bottom of the furnace. XRD examination of a sintered chip from each of the pellets showed them to be single-phase spinel. The pellets were then annealed at 800 °C for 853 h and then quenched by dropping the pellets from the furnace onto SiO_2 glass wool, which formed the lining of a previously evacuated metal beaker. As a cross-calibration, the cell parameter determined by Guinier X-ray diffraction, using NBS Si as an internal standard, was 8.0836 ± 0.0003 Å. The result of O'Neill (1997) indicates an MgO:Al_2O_3 ratio of 1:0.998(3), i.e., exactly stoichiometric within the error of the cell parameter determination. A second sample was synthesized in the same manner, but annealed at 900 °C for 96 h and made deliberately deficient in MgO with a composition of $Mg_{0.99}Al_2O_4$.

The neutron powder diffraction data were collected at high temperatures using time of flight diffractometers at the IPNS (Argonne National Laboratory, U.S.A.) and ISIS (Rutherford Appleton Laboratory, U.K.) spallation neutron sources. These diffractometers are described by Jorgensen et al. (1989) and Hull et al. (1992), respectively. A fixed scattering geometry and a relatively high flux at the detector with low background characterize these instruments, which allow rapid data collection from large thermally stable samples that can be heated to extreme temperatures (up to 2000 °C at ISIS) with f_{O_2} buffering, if needed.

Data for both the stoichiometric and Mg-deficient spi-

nels were collected from room temperature to 1400 °C on both heating and cooling at the special environment powder diffractometer (SEPD) at the intense pulsed neutron source (IPNS), using a rod-element resistance furnace and detectors in the 90° scattering position. The entire stack of sample pellets was positioned as a pile, held down by a weighted plunger within the furnace, which was evacuated to prevent oxidation of the furnace elements. The temperature was measured and controlled using type K thermocouples. The sample and furnace thermal mass ensured good thermal stability throughout each data collection. The neutron diffraction patterns were collected for a range of flight times corresponding to *d*-spacings between 0.4 and 3.2 Å. Each pattern was collected with a counting time of approximately 40 min. Additional heating experiments were conducted at the POLARIS diffractometer at ISIS, up to a temperature of 1600 °C, using a Ta cylindrical foil element resistance heater. This range of data included around 250 independent Bragg reflections, giving 140 individual Bragg peaks in the powder diffraction pattern when accounting for different reflections having identical *d*-spacings. The data from individual detectors were corrected for electronic noise, normalized against standard spectra from a sample of V, and focused using in-house software. No corrections were made for beam attenuation by the furnace or sample, because these were found to be negligible. We found no evidence for oxidation of the sample, which is unsurprising considering the high-temperature stability of $MgAl_2O_4$, the relatively high vacuum of the sample chamber and the close proximity of Ta and V metal to the sample, both of which act as oxygen getters.

The crystal structures were refined using the GSAS Rietveld refinement software (Larson and Von Dreele 1994). Total site occupancies were constrained to stoichiometric values completely describing the Mg-Al distribution. Scattering lengths of 5.375, 3.449, and 5.803 fm were used for Mg, Al, and O, respectively. The background was modeled using a sixth-order polynomial. The crystallographic variables were the unit-cell parameter, the coordinates of the oxygen atom, the occupancies of the tetrahedral and octahedral sites, and the isotropic temperature factors. The cell parameter was independently calibrated by cross calibrating against that determined from an aliquot of the same sample measured using X-ray diffraction with a Guinier camera and employing NBS Si as an internal standard. It was refined as 8.0836 ± 0.0002 Å. This value is expected for a stoichiometric sample that has been annealed and quenched according to our synthesis route (Navrotsky et al. 1986; O'Neill 1997). A typical neutron diffraction pattern is shown, together with the fit from the refinement, in Figure 1.

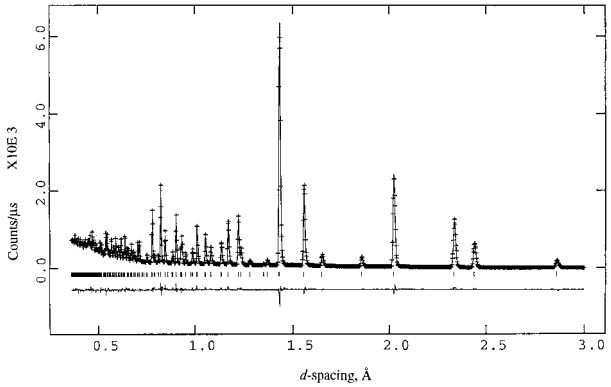

FIGURE 1. Time-of-flight neutron diffraction pattern for synthetic $MgAl_2O_4$ together with the calculated pattern and difference plot from Rietveld refinement. Note the high quality of the neutron diffraction data at low *d*-spacings.

RESULTS

The results of the high-temperature structural refinements for stoichiometric $MgAl_2O_4$ are given in Table 1. The essential feature of the structural response to temperature of interest to us is the exchange of metal cations between the tetrahedral and octahedral sites, which is given by the inversion parameter (equal to the occupancy of Al in the tetrahedral site). The temperature-dependence of the inversion and order parameters behavior are shown in Figure 2. The first heating and cooling runs were measured using SEPD at IPNS, although the second heating run was measured several months later using POLARIS at ISIS. The behavior takes the same form as that now observed in a number of minerals undergoing cation ordering (Redfern et al. 1996, 1997; Harrison et al. 1998a). The initial Q of around 0.67, corresponds to the degree of order quenched in from the initial sample synthesis. On the first heating run, the sample initially shows no change in the degree of order, until the temperature becomes high enough that exchange of Mg and Al between tetrahedral and octahedral sites (a thermally activated process) can commence. At this point (around 850 K) the sample begins to move toward its equilibrium state, which is a more ordered state. This relaxation toward a more ordered configuration is a kinetically controlled process. By 980 K, the sample has ordered on heating to a maximum degree of order with $Q \approx 0.78$, at which point it is essentially in equilibrium, and on further heating the sample progressively disorders down the equilibrium pathway. The cooling rate in the diffractometer is slower than that in the initial quench, so that the degree of order frozen in on the cooling path (to a value of around 0.79) is greater than that initially displayed. The subsequent heating pathway now follows the slow cooling pathway in reverse, corresponding to equilibrium degrees of order at temperatures of around 1000 K and above.

This behavior sheds light on some of the earlier studies of spinel that suggested the existence of a phase transition at temperatures between 600 and 700 °C. This is the temperature range over which the structure shows most change, due to relaxation of the ordering scheme on heating. Thus, the anomalous thermal expansion observed by Suzuki and Kumazawa (1980) at this temperature is due to structural adjustments occurring during the cation or-

TABLE 1. Refined structural parameters of $MgAl_2O_4$

T (K)	a (Å)	x	u	U_{iso} (oxy)	U_{iso} (tet)	U_{iso} (oct)	R_{wp}*
299†	8.08360(6)	0.218(8)	0.261714(35)	0.505(11)	0.219(21)	0.288(21)	0.085
683	8.11006(6)	0.196(10)	0.261642(45)	0.771(14)	0.632(34)	0.637(30)	0.085
707	8.11142(6)	0.178(10)	0.261644(46)	0.834(15)	0.671(35)	0.587(30)	0.084
766	8.11590(5)	0.189(10)	0.261672(44)	0.883(15)	0.681(34)	0.696(30)	0.084
837	8.12066(6)	0.184(10)	0.261594(46)	0.933(15)	0.808(37)	0.730(31)	0.084
903	8.12577(6)	0.169(10)	0.261735(46)	0.966(15)	0.858(38)	0.866(33)	0.083
969	8.13098(6)	0.146(10)	0.261972(47)	0.997(16)	0.985(41)	0.865(34)	0.083
1035	8.13564(6)	0.160(10)	0.261689(48)	1.114(17)	1.081(42)	0.895(34)	0.081
1100	8.13979(6)	0.199(11)	0.261437(49)	1.206(17)	1.118(44)	0.982(35)	0.080
1164	8.14426(6)	0.222(11)	0.261307(52)	1.292(19)	1.167(47)	1.070(37)	0.081
1228	8.14888(6)	0.206(11)	0.261121(53)	1.382(19)	1.345(50)	1.111(38)	0.080
1291	8.15365(6)	0.234(11)	0.260954(54)	1.472(20)	1.406(53)	1.170(39)	0.079
1355	8.15805(6)	0.236(13)	0.260943(62)	1.538(23)	1.470(61)	1.194(44)	0.088
1418	8.16360(6)	0.249(12)	0.260701(61)	1.706(23)	1.570(61)	1.304(44)	0.083
1481	8.16885(6)	0.271(12)	0.260582(60)	1.695(24)	1.561(61)	1.338(44)	0.082
1544	8.17402(6)	0.268(12)	0.260506(61)	1.779(24)	1.755(65)	1.384(45)	0.082
1606	8.17940(6)	0.286(12)	0.260328(63)	1.868(25)	1.759(66)	1.426(45)	0.082
1644	8.18326(6)	0.294(12)	0.260284(63)	1.937(25)	1.769(66)	1.517(46)	0.080
1662	8.18536(6)	0.298(12)	0.260292(64)	1.982(26)	1.928(70)	1.567(47)	0.081
1650‡	8.18455(6)	0.296(12)	0.260345(62)	1.918(25)	1.762(66)	1.601(46)	0.078
1595	8.17903(6)	0.275(12)	0.260318(63)	1.875(25)	1.769(66)	1.490(47)	0.082
1532	8.17360(6)	0.277(12)	0.260519(60)	1.769(23)	1.638(61)	1.399(44)	0.080
1468	8.16810(6)	0.279(12)	0.260538(59)	1.689(23)	1.557(60)	1.417(43)	0.081
1405	8.16459(6)	0.245(16)	0.260656(81)	1.658(31)	1.576(83)	1.224(59)	0.117
1278	8.15030(6)	0.214(24)	0.26089(11)	1.447(43)	1.55(11)	1.107(83)	0.181
1214	8.14730(6)	0.207(11)	0.261054(53)	1.400(19)	1.275(49)	1.073(38)	0.080
1152	8.14249(6)	0.202(11)	0.261257(52)	1.332(19)	1.221(48)	1.039(37)	0.081
1088	8.13777(6)	0.199(11)	0.261430(50)	1.228(18)	1.168(46)	1.017(36)	0.082
1024	8.13316(6)	0.196(11)	0.261627(49)	1.148(17)	1.054(44)	1.013(36)	0.082
961	8.12854(6)	0.154(10)	0.261833(47)	1.055(16)	0.979(41)	0.831(34)	0.083
898	8.12390(6)	0.132(10)	0.262026(45)	0.946(15)	0.919(38)	0.807(33)	0.083
834	8.11928(6)	0.127(10)	0.262127(45)	0.868(15)	0.873(38)	0.747(32)	0.085
770	8.11468(6)	0.126(10)	0.262104(45)	0.820(14)	0.772(36)	0.720(32)	0.087
710	8.11057(6)	0.140(11)	0.262098(49)	0.789(15)	0.688(37)	0.653(34)	0.096
610	8.10563(6)	0.133(10)	0.262088(45)	0.730(14)	0.612(34)	0.584(31)	0.093
516	8.09701(5)	0.139(10)	0.262142(41)	0.603(12)	0.467(29)	0.482(27)	0.090
464	8.09365(5)	0.137(10)	0.262155(41)	0.563(12)	0.463(28)	0.447(27)	0.092
405	8.09159(6)	0.143(11)	0.262132(46)	0.514(13)	0.365(30)	0.439(30)	0.105
298§	8.08360(6)	0.143(10)	0.262015(31)	0.491(9)	0.424(22)	0.185(19)	0.053
473	8.09650(6)	0.137(10)	0.261986(31)	0.675(10)	0.634(25)	0.354(21)	0.049
673	8.11009(6)	0.155(11)	0.261981(32)	0.865(11)	0.836(27)	0.575(23)	0.046
773	8.11685(6)	0.145(10)	0.261992(32)	0.958(11)	0.960(28)	0.643(24)	0.048
873	8.12443(6)	0.131(11)	0.262150(32)	1.044(11)	1.072(29)	0.758(25)	0.043
973	8.13192(6)	0.137(11)	0.262088(33)	1.172(12)	1.204(31)	0.836(25)	0.042
1073	8.13916(6)	0.163(11)	0.261790(34)	1.333(12)	1.316(32)	0.950(26)	0.040
1173	8.14652(6)	0.194(11)	0.261520(36)	1.484(13)	1.427(34)	1.089(27)	0.039
1273	8.15428(6)	0.205(11)	0.261333(36)	1.640(13)	1.638(36)	1.174(27)	0.037
1373	8.16214(6)	0.230(11)	0.261196(38)	1.810(14)	1.748(38)	1.337(28)	0.036
1473	8.17015(6)	0.236(11)	0.260967(39)	1.962(15)	1.905(40)	1.435(29)	0.036
1573	8.17859(6)	0.255(13)	0.260865(46)	2.108(17)	2.106(48)	1.568(34)	0.036
1673	8.19804(6)	0.298(11)	0.260545(43)	2.476(17)	2.341(46)	1.899(32)	0.032
1773	8.20091(6)	0.336(11)	0.260542(43)	2.501(16)	2.326(46)	1.996(32)	0.034
1873	8.20857(6)	0.347(12)	0.260482(43)	2.617(18)	2.398(50)	2.127(34)	0.035

* $R_{wp} = \Sigma w(F_{obs} - F_{calc})^2/\Sigma wI^2_{obs}$.
§ Data collected during heating at ISIS, Rutherford Appleton Laboratory, U.K.
† Data collected during heating at IPNS, Argonne National Laboratory, U.S.A.
‡ Data collected during cooling at IPNS.

dering relaxation, rather than being due to a further discrete phase transition.

A further, intriguing and rather subtle feature, can be seen in the temperature-dependence of the inversion parameter between 950 and 1150 K in the initial heating and cooling run, and is shown in the inset of Figure 2a. It appears that, at these temperatures, the sample may favor a degree of order of around 0.70. On heating, the degree of order suddenly drops from 0.76 (at around 1040 K) to 0.70 (at around 1100 K) in one heating step. This is lower than the equilibrium degree of order expected at 1100 K. Similarly, on cooling, the sample does not appear to order exactly along the equilibrium curve between around 1140 and 1020 K, but instead locks in to a degree of order of around 0.70. Then, on the next cooling step to approximately 960 K the sample suddenly orders to $Q \approx 0.76$. The value of 70% order, which appears to be the favored state over this temperature interval, is the degree of order in equilibrium at around 800 °C, the temperature at which the sample was annealed for more than 850

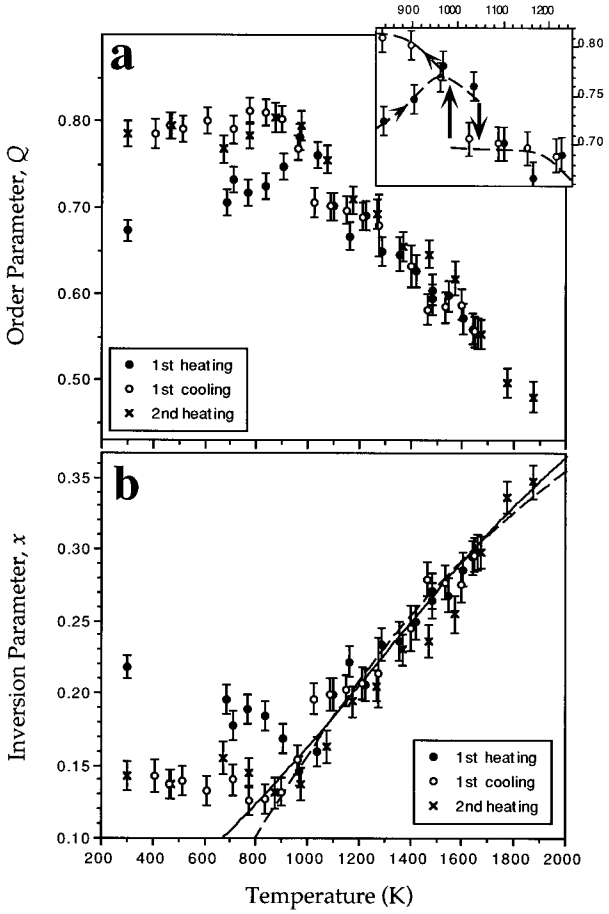

FIGURE 2. Temperature dependence of (**a**) the order parameter (Q) and (**b**) inversion parameter (x), for cation order-disorder in spinel, from in situ neutron diffraction. Circle = data obtained at IPNS; X = data obtained from the same sample during a subsequent in situ heating experiment at ISIS. The dashed line in **b** is a fit to the equilibrium data between 560 and 1600 °C using the O'Neill and Navrotsky (1983) thermodynamic model (Eq. 3), yielding $\alpha = +32.8 \pm 0.9$ kJ/mol and $\beta = +4.7 \pm 2.0$ kJ/mol. The solid line shows the fit to the Landau expression for ordering (Eq. 6) with values of $T_c = 445 \pm 109$ K and $c' = 1.62 \pm 0.21$.

hours. Taking account of the errors in the measurements, these observations of possible changes away from the equilibrium curve are on the limit of statistical significance (furthermore, they are not reflected in the behavior of the oxygen positional parameter). However, if they do reflect some real effect, then it could tentatively be explained if some other temperature-dependent structural feature is coupled to the order-disorder process, which then shows a memory of the annealing conditions. For example, maybe the sample has retained the equilibrium defect concentration from 800 °C and in our subsequent high-temperature experiment these defects then interact with the ordering states to create a local minimum in order parameter space at $Q \approx 0.70$. Thus, on heating, as Q approaches 0.70, the sample disorders to this value more rapidly than would otherwise be expected, and on cooling the degree of order sticks at this value (akin to supercooling) at temperatures when it would otherwise be expected to be more ordered. The hysteresis in the behavior is commensurate with $Q \approx 0.70$ being a local minimum. On the second heating run (conducted at ISIS) this effect is not obvious. Possibly because the sample was at ambient temperature for several months in between the two experiments, but also potentially because the temperature steps are more widely spaced. Although this behavior has not (to the authors' knowledge) been noted before for a non-convergent order-disorder process, it is reminiscent of the memory effect sometimes seen at symmetry-breaking phase transitions and typically observed in domain microstructures, as in quartz and anorthite at high temperature, for example see Xu and Heaney (1997).

The oxygen positional parameter, u, strongly correlates with the degree of order (Fig. 3), and shows an approximately linear relationship:

$$u = 0.26344 - 0.01021x. \quad (1)$$

In contrast, the cell parameters appear insensitive to the degree of order.

The bond-lengths at the tetrahedral and octahedral sites in spinel show interesting temperature evolution, because their temperature response involves two effects: thermal expansion and changing cation order (and hence Al/Mg occupancy) at the site. The cation-oxygen bond length as a function of temperature for $MgAl_2O_4$ (Fig. 4) shows that the tetrahedral site tends to *decrease* in size with increasing temperature, when an equilibrium degree of order exists, because the occupancy of the smaller Al^{3+} cation in that site increases with temperature. On the other hand, the expansion of the octahedral site with temperature is anomalously large because not only do the lengths of the individual Mg-O and Al-O bonds increase, but the occupancy of that site by the larger Mg^{2+} cation increases as well. Knowledge of the degree of order at each temperature allows determination of the thermal expansion of each type of cation in each coordination environment. The behavior of the bond lengths below 1000 K is dominated by relaxation of the structure toward an equilibrium cation distribution on heating (and by the departure from equilibrium on cooling below a blocking temperature for ordering). From Figure 2, the degree of cation order does not change below 800 K, and hence the thermal response up to that temperature can be interpreted as exclusively due to thermal expansion of the metal-oxygen bonds. Above 1000 K, the thermal evolution of the average bond lengths at the two sites reflects the combined effects of thermal expansion and changing cation order.

Table 2 gives data for non-stoichiometric $Mg_{0.99}Al_2O_4$ spinel. At all temperatures, $Mg_{0.99}Al_2O_4$ is more disordered than its stoichiometric counterpart by about $x \sim 0.02$. The temperature at which structural relaxation begins is slightly lower than in the stoichiometric $MgAl_2O_4$, in agreement with the finding that the kinetics of order-

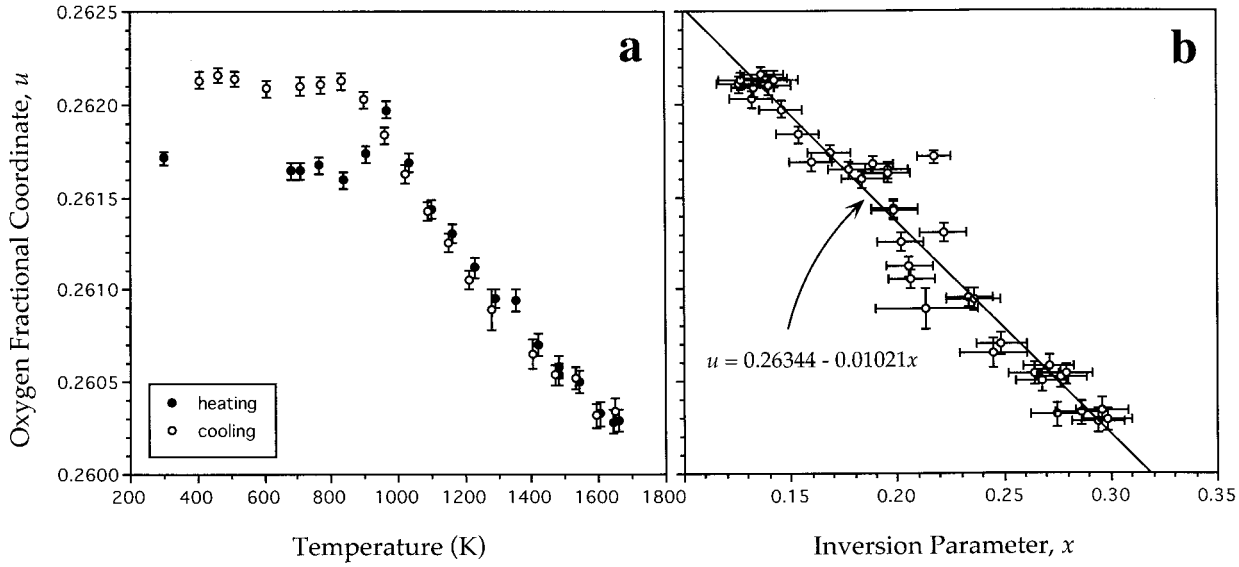

FIGURE 3. Oxygen positional parameter (u) as a function of temperature (**a**) and inversion parameter, x (**b**). Solid line is a least-squares fit to the data.

disorder in spinels is strongly dependent on defect concentration (O'Neill 1997), and is enhanced by vacancies.

DISCUSSION

Thermodynamic model

Several thermodynamic approaches to cation ordering in spinels exist (Navrotsky and Kleppa 1967; O'Neill and Navrotsky 1983, 1984; Carpenter et al. 1994; Carpenter and Salje 1994a, 1994b). We present here only a brief account of the three most commonly used thermodynamic models for cation ordering in spinels, before applying them to the observed cation ordering data.

The thermodynamic model described by O'Neill and Navrotsky (1983) expresses the enthalpy of a spinel with an intermediate cation distribution (relative to the same spinel with the normal cation distribution) as a quadratic function of the degree of inversion ($\Delta H = \alpha x + \beta x^2$). Although O'Neill and Navrotsky's (1983) lattice energy considerations suggested that this was the form of the enthalpy, they did not predict the sign of β, which could be negative or positive. For the sake of simplifying models of spinel solid solutions, β is frequently assumed negative for all 2–3 spinels, with a value of around −20 kJ/mol. The free energy of ordering is given by combining this excess enthalpy with the configurational entropy of the intermediate cation distribution:

$$\Delta G = \alpha x + \beta x^2 + RT \sum_{i,j} N_j X_i^j \ln X_i^j \qquad (2)$$

where X_i^j is the fraction of cation i on site j, and N_j is the number of j-sites per formula unit. The equilibrium pathway of x is given by $\partial \Delta G/\partial x = 0$, which gives the expression:

$$-RT \ln\left(\frac{x^2}{(1-x)(2-x)}\right) = \alpha + 2\beta x. \qquad (3)$$

This expression has been shown to provide a good description of the temperature-dependent ordering behavior of a wide range of 2–3 spinels (Wu and Mason 1981; Nell et al. 1989; O'Neill et al. 1991, 1992; O'Neill 1992, 1994; Harrison et al. 1998a). Previous attempts to describe cation ordering in $MgAl_2O_4$ yielded values for the free parameters of $\alpha = 35$ kJ, $\beta = -32$ kJ (Maekawa et al. 1997); $\alpha = 31$ kJ, $\beta = -10$ kJ (Peterson et al. 1991); and $\alpha = 25$ kJ, $\beta = 6$ kJ (Millard et al. 1992). Clearly significant discrepancy exists among the described behav-

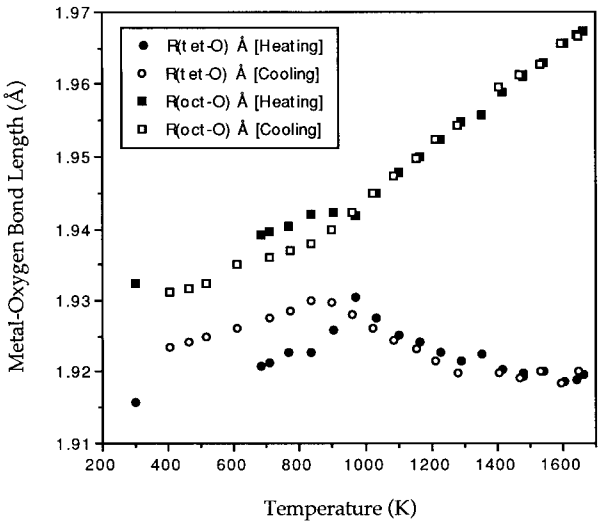

FIGURE 4. Behavior of the metal-oxygen bond lengths at the tetrahedral (circles) and octahedral (squares) sites on heating (filled) and cooling (open). The temperature variation of the bond length is controlled by both the temperature variation of the site occupancies and the individual thermal expansions of the Mg-O and Al-O bonds in tetrahedral and octahedral coordination.

TABLE 2. Refined structural parameters for $Mg_{0.99}Al_2O_4$ (data collected at IPNS)

T (K)	a (Å)	x	u	U_{iso} (oxy)	U_{iso} (tet)	U_{iso} (oct)	R_{wp}*
364†	8.09580(5)	0.199(9)	0.261728(37)	0.500(11)	0.288(24)	0.360(23)	0.084
374	8.09613(6)	0.186(10)	0.261750(44)	0.515(13)	0.300(28)	0.331(27)	0.099
420	8.09924(6)	0.189(10)	0.261675(44)	0.552(13)	0.339(29)	0.400(28)	0.097
502	8.10384(6)	0.193(10)	0.261701(45)	0.608(13)	0.420(30)	0.454(29)	0.094
563	8.10870(6)	0.186(10)	0.261725(45)	0.671(14)	0.506(32)	0.502(30)	0.094
636	8.11359(6)	0.170(10)	0.261666(46)	0.745(15)	0.602(34)	0.545(30)	0.092
707	8.11850(6)	0.185(11)	0.261610(48)	0.799(15)	0.622(36)	0.647(33)	0.093
778	8.12333(6)	0.196(11)	0.261653(48)	0.843(16)	0.672(37)	0.714(33)	0.091
848	8.12816(6)	0.185(11)	0.261674(48)	0.815(11)	0.713(38)	0.754(34)	0.088
916	8.13321(6)	0.156(11)	0.261773(49)	0.957(17)	0.897(41)	0.785(35)	0.088
984	8.13801(6)	0.182(11)	0.261559(49)	1.043(17)	0.935(42)	0.799(35)	0.085
1080	8.14282(7)	0.201(11)	0.261410(52)	1.130(18)	1.074(46)	0.895(37)	0.087
1116	8.14757(7)	0.236(11)	0.261158(54)	1.266(19)	1.070(48)	0.882(38)	0.085
1182	8.15239(7)	0.252(11)	0.260957(55)	1.319(20)	1.087(50)	1.089(40)	0.086
1232	8.15738(7)	0.242(12)	0.260780(57)	1.427(21)	1.321(54)	1.072(40)	0.084
1311	8.16234(7)	0.286(12)	0.260710(59)	1.513(22)	1.212(55)	1.188(42)	0.084
1376	8.16775(7)	0.269(12)	0.260599(61)	1.614(23)	1.508(60)	1.226(44)	0.084
1441	8.17306(7)	0.283(12)	0.260465(62)	1.682(24)	1.547(62)	1.303(45)	0.083
1506	8.17838(7)	0.287(12)	0.260414(64)	1.757(25)	1.621(65)	1.353(46)	0.083
1573	8.18394(7)	0.301(12)	0.260198(65)	1.863(26)	1.651(66)	1.375(47)	0.083
1639	8.18961(8)	0.320(14)	0.259994(72)	1.995(28)	1.767(75)	1.533(52)	0.087
1676	8.19344(7)	0.288(13)	0.259903(69)	2.016(27)	1.896(71)	1.451(48)	0.081
1671‡	8.19336(7)	0.323(13)	0.259992(67)	2.014(26)	1.805(70)	1.564(49)	0.080
1622	8.18850(7)	0.293(13)	0.260242(66)	1.936(26)	1.915(71)	1.454(48)	0.082
1557	8.18299(7)	0.300(12)	0.260268(64)	1.821(25)	1.655(65)	1.392(46)	0.081
1492	8.17760(7)	0.302(12)	0.260437(62)	1.730(24)	1.532(63)	1.413(46)	0.081
1427	8.17236(7)	0.288(12)	0.260478(61)	1.672(23)	1.508(61)	1.339(45)	0.082
1362	8.16703(7)	0.280(12)	0.260656(60)	1.591(23)	1.397(58)	1.202(43)	0.083
1299	8.16204(7)	0.262(12)	0.260836(57)	1.493(22)	1.350(55)	1.131(41)	0.084
1235	8.15701(7)	0.258(12)	0.260873(56)	1.427(21)	1.228(52)	1.069(40)	0.083
1171	8.15222(7)	0.232(11)	0.261034(54)	1.334(20)	1.200(50)	1.046(39)	0.083
1107	8.14740(7)	0.220(11)	0.261188(54)	1.245(19)	1.132(49)	1.009(39)	0.085
1043	8.14254(6)	0.200(11)	0.261382(51)	1.122(18)	1.010(44)	0.874(36)	0.086
978	8.13806(6)	0.198(11)	0.261535(50)	1.049(17)	0.934(43)	0.831(36)	0.085
913	8.13333(6)	0.179(11)	0.261729(49)	0.964(17)	0.863(41)	0.776(35)	0.087
834	8.12870(6)	0.161(11)	0.261886(48)	0.888(16)	0.831(39)	0.722(34)	0.089
783	8.12406(6)	0.150(11)	0.261920(47)	0.813(15)	0.724(37)	0.658(33)	0.090
718	8.11961(6)	0.177(10)	0.261906(46)	0.773(15)	0.617(35)	0.621(32)	0.091
654	8.11512(6)	0.171(10)	0.261977(44)	0.705(14)	0.604(33)	0.561(30)	0.090
591	8.11084(6)	0.172(10)	0.262002(44)	0.636(14)	0.546(33)	0.512(30)	0.094
530	8.10662(6)	0.171(10)	0.261961(44)	0.607(13)	0.460(31)	0.491(29)	0.095
430	8.10285(6)	0.155(10)	0.261961(44)	0.570(13)	0.402(29)	0.426(28)	0.096
368	8.10120(11)	0.184(18)	0.262102(78)	0.555(23)	0.383(52)	0.403(50)	0.174

* $R_{wp} = \Sigma w(F_{obs} - F_{calc})^2/\Sigma wI^2_{obs}$.
† Heating cycle.
‡ Cooling cycle.

iors, not least because of the experimental difficulties in determining cation site occupancies at high temperature with accuracy, combined with the generally small temperature ranges over which the order-disorder was measured in the past. Our new high-temperature neutron data, however, provide a unique opportunity to re-appraise the models of the ordering behavior with more reliability than has been possible previously. They provide an absolute and precise measure of the long-range order in spinel over a very wide temperature range all the way up to 1600 °C.

A multiple non-linear least-squares fit to the equilibrium behavior of the inversion parameter from the data of stoichiometric $MgAl_2O_4$ measured at both ISIS and IPNS (between 560 °C and 1600 °C) yields values of the thermodynamic parameters $\alpha = +32.8 \pm 0.9$ kJ/mol and $\beta = +4.7 \pm 2.0$ kJ/mol, with a reduced χ^2 of 1.46. The data were weighted according to estimated standard deviations from the refinements quoted in Table 1, and an estimated uncertainty in the temperature of ±5 °C. The result (Fig. 2b) provides a good fit to the data, but the sign of the refined β parameter is opposite to that found in many other 2–3 spinels and most other (more limited and lower resolution) data sets for $MgAl_2O_4$ analyzed using this model. It does, however, reflect the recent findings for hercynite reported by Harrison et al. (1998a). It appears that the assumption that cation ordering in all 2–3 spinels can be described by an expression for enthalpy with a constant value of $\beta = -20$ kJ/mol is not justified.

An alternative expression for the free energy of ordering, truncates the enthalpy at the linear term in x, but incorporates an additional term for the entropy, to account for any non-configurational entropy:

$$\Delta G = ax - T\sigma x + RT \sum_{i,j} N_j X_i^j \ln X_i^j. \qquad (4)$$

Fitting the data, as before, we obtain $\alpha = 30.7 \pm 1.1$ kJ

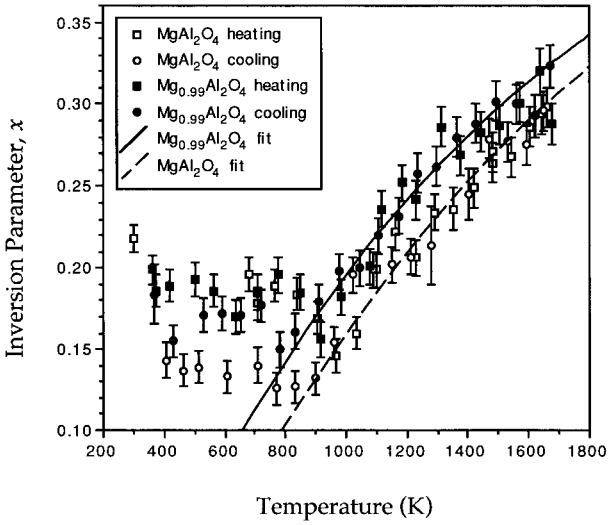

FIGURE 5. Comparison of the temperature variation of the inversion parameter, *x*, in stoichiometric (open symbol) and slightly non-stoichiometric spinel (filled symbols). The effect of Mg-deficiency is to decrease the overall degree of order. The solid line and dashed lines are fits to the data for the two compositions using O'Neill and Navrotsky's (1983) thermodynamic model.

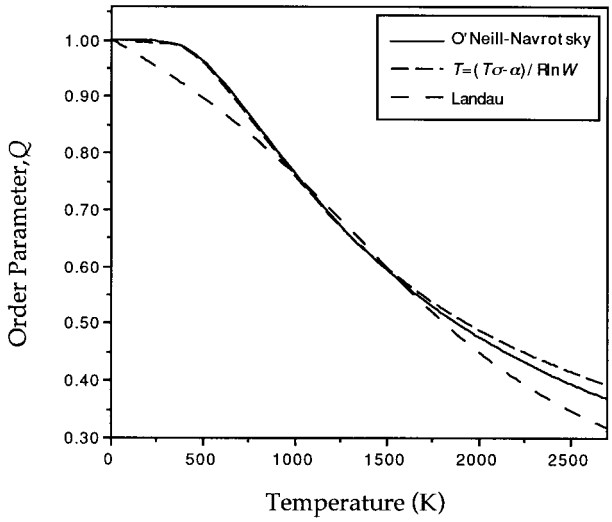

FIGURE 6. Comparison of the three models for the free energy of order-disorder in spinel, over a wide temperature interval. Extrapolation beyond the temperature range of the fitted data leads to significant discrepancies in the expected order-disorder behavior.

and $\sigma = -3.22 \pm 0.80$ J with a reduced χ^2 of 1.44. The fit is, therefore, as good as that given by Equation 3, but (at the temperatures corresponding to our data) the negative value of σ means that the $-T\sigma x$ term in the expression for free energy is approximately equivalent to the βx^2 term in Equation 2.

Another approach to modeling ordering in spinels proposed by Carpenter et al. (1994) and Carpenter and Salje (1994a) is based on Landau's theory of phase transitions (Landau and Lifshitz 1980): The free energy of an intermediate spinel is calculated relative to a hypothetical spinel with the fully disordered cation distribution. The excess free energy of ordering is expressed as an expansion in terms of the order parameter, *Q*:

$$\Delta G = -\mathrm{h}Q + \frac{1}{2}\mathrm{a}(T - T_c)Q^2 + \frac{1}{6}\mathrm{c}Q^6 \qquad (5)$$

where h, a, T_c, and c are constants. This expression for the free energy differs from that given in Equation 2 in two respects. First, the ΔH term in the Landau expansion contains linear, quadratic, and 6th-order terms, whereas ΔH in Equation 2 is expressed as linear and quadratic terms. Second, the excess entropy of ordering in the Landau potential is a simple quadratic function of the order parameter, in contrast to the exact form of the configurational entropy employed in the O'Neill and Navrotsky (1983) model and the expression given in Equation 4.

Setting $\partial\Delta G/\partial Q = 0$, an expression relating *Q* and *T* at equilibrium is obtained:

$$T = T_c + \frac{T_c}{(\mathrm{c}' - 1)Q}(1 - \mathrm{c}'Q^5) \qquad (6)$$

where $\mathrm{c}' = \mathrm{c}/\mathrm{h}$ (Harrison and Putnis 1997). A weighted least squares fit (employing the errors for *Q* given by the refinements and errors in *T* of ± 5 K) of the data of stoichiometric $MgAl_2O_4$ (for the 38 measurements between 560 and 1600 °C) yields values of the thermodynamic parameters of $T_c = 445 \pm 109$ K and $\mathrm{c}' = 1.62 \pm 0.21$, with a reduced χ^2 of 1.36. Comparing the fit of the Landau model with the O'Neill-Navrotsky model for ordering (Fig. 2), we see that both formalisms fit the measured data adequately over the temperature interval of the data. At the temperatures of geological interest, the curvature of the O'Neill-Navrotsky ordering scheme is greater than that of the Landau model, and the curvature of the ordering scheme described by Equation 4 is greatest of all. These descriptions will differ more markedly from each other on extrapolation outside the range of the fitted data, for example at conditions close to the melting point of $MgAl_2O_4$ (Fig. 6).

Data from the non-stoichiometric Mg-deficient spinel, $Mg_{0.99}Al_2O_4$ were fit using the same thermodynamic models and procedures. Equation 2 yields $\alpha = +25.7 \pm 1.4$ kJ/mol and $\beta = +11.4 \pm 2.8$ kJ/mol, with a reduced χ^2 of 0.85 (shown in Fig. 5). Equation 4 gives $\alpha = 24.3 \pm 1.2$ kJ and $\sigma = -5.68 \pm 0.95$ J with a reduced χ^2 of 0.80. Fitting to the Landau expression for the ordering behavior (Eq. 6) gives parameters of $T_c = -122 \pm 151$ K and $c' = 0.87 \pm 0.15$, with a reduced χ^2 of 0.95. Comparing the fitted equilibrium behavior of the $MgAl_2O_4$ with that of $Mg_{0.99}Al_2O_4$, we see that the effect of introducing 1 mol% Mg deficiency into the structure is to increase the degree of inversion by $x \approx 0.02$.

Comparison with earlier studies on $MgAl_2O_4$

Our work is unique in that it gives an absolute measure of the average cation site occupancies over a greater tem-

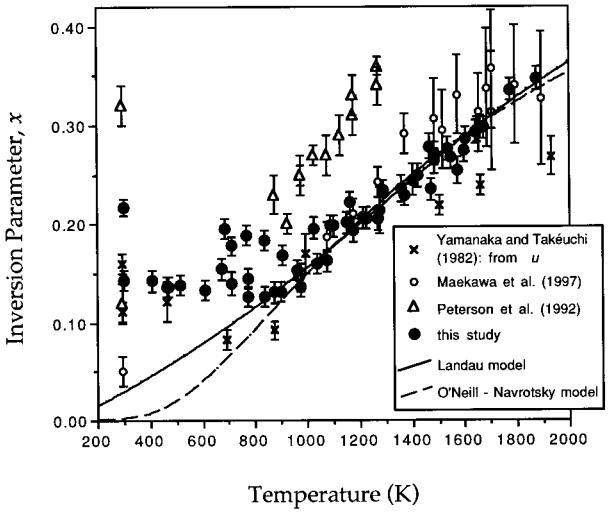

FIGURE 7. Comparison of our data (solid circles) with earlier studies of order-disorder in spinel. Yamanaka and Takéuchi's (1982) values of *u*, combined with our result from Figure 3b, were used to infer a measurement of *x* from their X-ray study.

perature range than any previous in situ study, and with the finest temperature resolution yet attained (Fig. 7). There are three high-temperature in situ studies of order-disorder in spinel that we may compare our results against, to reveal a consistent picture of the high-temperature behavior.

The single-crystal X-ray study of Yamanaka and Takéuchi (1983) reported anomalously low occupancies of Al in the tetrahedral site, suggesting that spinel was more ordered at high temperature than found here. Part of the difficulty of obtaining site occupancies from X-ray diffraction is that there is almost no scattering contrast between Mg and Al, and site occupancies cannot be determined absolutely and reliably by this method. Yamanaka and Takéuchi did, however, report values for the oxygen positional parameter as a function of temperature for their sample. Furthermore, our neutron results define the relationship between oxygen positional parameter, *u*, and inversion parameter, *x*. Thus, using Equation 1 (above), we can convert Yamanaka and Akeuchi's values of *u* into equivalent values for the inversion parameter, *x*. This gives the disordering behavior shown by the crosses in Figure 7. Although similar to our results, their data would still suggest that the sample was more ordered than we would expect at high temperatures. This may be due to the low values of *x* that they use in their crystal structure refinements, because our Rietveld refinements show that the values of *u* and *x* are correlated to some extent. It would be interesting to refine the data of Yamanaka and Takéuchi once again, imposing more realistic values for *x* on the refinement, because this is likely to reduce *u* to a value that is in closer agreement with our results.

The neutron diffraction work of Peterson et al. (1991) followed a similar approach to our work, but (as can be seen from their data, shown as triangles in Fig. 7) suggests spinel is more disordered than seen here. This likely occurs because their samples were non-stoichiometric: as we have shown, a small degree of non-stoichiometry introduces a significant degree of additional disorder. Unfortunately, they do not provide a value of the cell parameter of their samples that was obtained using an internal standard, and the cell parameter obtained by time-of-flight neutron diffraction is dependent, at the level of one part in 10000, on the exact position of the sample in the flight path and the calibration of the detectors. We would expect results similar to those obtained by Peterson et al. (1991) for a spinel sample of approximate composition $Mg_{0.96}Al_2O_4$.

High-temperature NMR work of Maekawa et al. (1998) provides new in situ measurements of the inversion parameter up to the highest temperatures of our study (1600 °C). The open circles show their results in Figure 7. We see that their results are in good agreement with our measurements across the temperature range. It is interesting to note, therefore, that they obtained quite different results for a fit to their data of the O'Neill and Navrotsky (1983) model, which they reported as gave $\alpha = 35 \pm 5$ kJ, $\beta = -32 \pm 5$ kJ when applied to their data. It appears, however, that they used an unweighted fit to obtain their parameters. We suggest that the difference between their conclusions and ours, regarding the thermodynamic modeling of the disordering process, lies in the large errors associated with their highest temperature data. These data exert a strong leverage on the fitted results, especially if an unweighted fit is attempted. On the other hand, we have high confidence in all our refined site occupancies, up to the highest temperature of study, and (carrying out a properly weighted fit) obtain a small positive value for β, rather than the large negative value suggested by Maekawa et al. (1998). This serves as a caveat for the fitting of such models to order-disorder data, because the fit parameters (especially second-order terms such as the β term in Eq. 2) can have a high sensitivity to the data at the extreme end of the measurement range. In conclusion, we note that Figure 7 indicates that our results are consistent with the previous in situ studies of $MgAl_2O_4$ ordering in spinel, but provide a new thermodynamic description for the disordering behavior in which we can feel confident.

Kinetic behavior

The process of cation distribution relaxation, which occurs when quenched materials are heated slowly to high temperatures, has been quantified by Harrison and Putnis (1996) and Redfern et al. (1996) using the Ginzburg-Landau rate law (Carpenter and Salje 1989; Salje 1988). The rate law is of the form:

$$\frac{dQ}{dt} = -\frac{\gamma \exp(-\Delta H^*/RT)}{2RT}\frac{\partial \Delta G}{\partial Q} \qquad (7)$$

where t is time, γ is a frequency factor, ΔH^* is the activation energy, and ΔG is the appropriate free energy po-

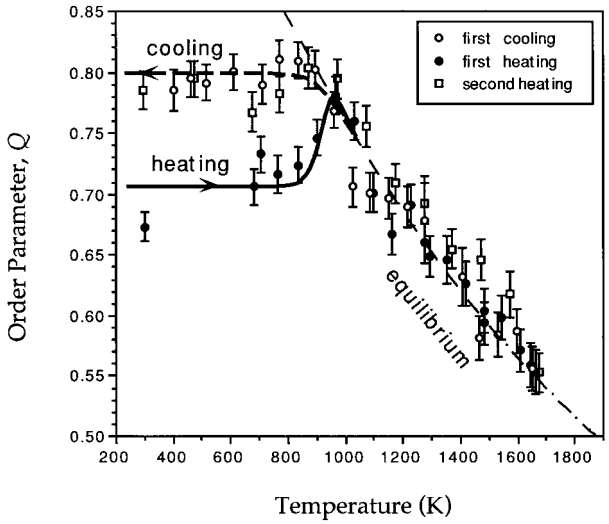

FIGURE 8. Calculation of the cation distribution relaxation process with a heating rate of 60 K/h. Thick lines are the calculated non-equilibrium behavior using the Ginzburg-Landau rate law (Eq. 7) on heating (solid) and cooling (dashed), with the thermodynamic driving force given by the O'Neill and Navrotsky (1983) model (Eq. 2). Thin dashed line = the equilibrium ordering curve from Equation 2.

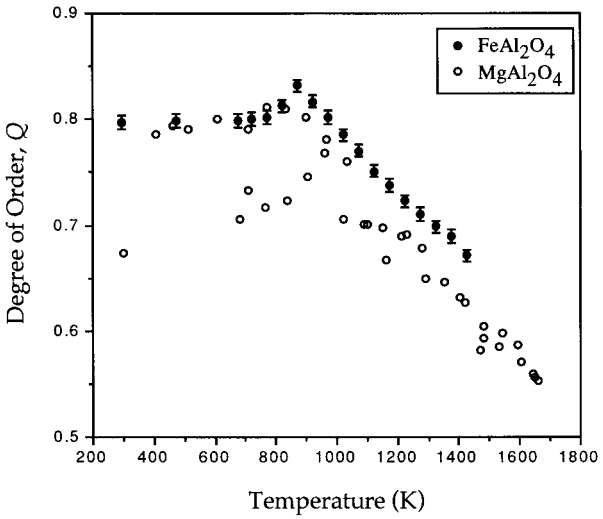

FIGURE 9. Comparison of the high-temperature order-disorder behavior of spinel (this study, shown as open circles) with that of hercynite (solid circles, data of Harrison et al. 1998). The close correspondence between the temperature-dependent behavior of the end-members indicates the ideality of the spinel-hercynite solid solution.

tential describing the cation ordering process. Integrating Equation 7 under isothermal conditions we obtain:

$$t - t_0 = \int_{Q_0}^{Q} \frac{-2RT}{\gamma \exp(-\Delta H^*/RT)} \left(\frac{\partial \Delta G}{\partial Q}\right)^{-1} dQ \qquad (8)$$

where Q_0 is the initial value of Q at time t_0. This allows one to calculate the time taken to change Q by $\Delta Q = Q - Q_0$. Alternatively (and more usefully) an inverse calculation may be made and the time dependence of the relaxation of Q toward equilibrium may be found: The change in Q, $Q - Q_0$, expected during a time interval $t - t_0$, can be determined by calculating the integral numerically over a range of limits of Q, and iteratively obtaining the best fit value of Q corresponding to t. Alternatively one may calculate the change in Q for a given annealing time by evaluating Equation 8 numerically, and varying the upper limit of integration in an iterative procedure until the correct annealing time is obtained. The evolution of Q vs. t during heating or cooling at a constant rate can be determined by approximating the constant heating or cooling rate by a series of discrete isothermal annealing steps separated by an instantaneous temperature change.

To apply the O'Neill and Navrotsky (1983) model to the Ginzburg-Landau rate law, the free energy due to ordering (Eq. 2) was recast in terms of Q, using the symmetric formalism of Holland and Powell (1996). An estimate for the frequency factor $\gamma = 1.354 \times 10^9$ s^{-1} was taken from the analysis of the kinetics of order-disorder in $MgFe_2O_4$ spinel (Harrison 1997). The activation energy was then chosen in order to fit the experimental data. A value of $\Delta H^* = 230$ kJ/mol gave the best fit, although our confidence in this value can only be as high as our confidence in the choice of γ. The kinetic calculation was performed with a heating rate of 60 K/h, which was the approximate heating rate used during the neutron data collection. The constant heating rate was approximated to a series of isothermal annealing steps of 72 s duration, separated by an instantaneous temperature increase of 1 K. The calculation was begun at room temperature and $Q = 0.706$ (i.e., the degree of order maintained after quenching from the synthesis temperature). The calculated evolution of Q vs. T during heating is shown in Figure 8.

Implications for ordering in the $Mg_xFe_{1-x}Al_2O_4$ solid solution

In Figure 9 we compare the results of this study with a recent in-situ neutron diffraction study of ordering in $FeAl_2O_4$ (Harrison et al. 1998a). The degree of inversion as a function of temperature in the Mg and Fe end-members is identical within the error. The thermodynamic coefficients obtained by Harrison et al. (1998a) are $\alpha = 31.3$ kJ/mol and $\beta = 19.7$ kJ/mol, which supports the conclusion made earlier that β is not negative for all spinels. The close correspondence between the temperature dependent behavior of the end-members indicates the ideality of the spinel-hercynite solid solution. O'Neill et al. (1992), in their comparison of ordering in magnesioferrite ($MgFe_2^{3+}O_4$) and magnetite ($Fe^{2+}Fe_2^{3+}O_4$), reached the same conclusion regarding the similarity of Mg and Fe^{2+} in 2–3 spinels. This allows use of simplifying assumptions to model the thermodynamics of the Mg-Al-Fe^{2+}-Fe^{3+} spinel system (Harrison et al. 1998b).

ACKNOWLEDGMENTS

This work was carried out with the support of the Natural Environment Research Council, grant no. GR9/02917 and beam time support from IPNS, Argonne. The authors thank Ron Smith and Simine Short for their help in performing the neutron scattering experiments. R.J.H. gratefully acknowledges the support of the Alexander von Humboldt-Stiftung.

REFERENCES CITED

Brun, E. and Hafner, S. (1962) Die elektrische Quadrupolaufsplatung von Al^{27} in Spinell $MgAl_2O_4$ und Korund Al_2O_3. I. Paramagnetische Kernresonanz von Al^{27} und Kationenverteilung in Spinell. Zeitshrift für Kristallographie, 117, 37–62.

Carpenter, M.A. and Salje, E.K.H. (1989) Time-dependent Landau theory for order/disorder processes in minerals. Mineralogical Magazine, 53, 483–504.

———(1994a) Thermodynamics of nonconvergent cation ordering in minerals: II. Spinels and the orthopyroxene solid solution. American Mineralogist, 79, 1068–1083.

———(1994b) Thermodynamics of nonconvergent cation ordering in minerals: III. Order parameter coupling in potassium feldspar. American Mineralogist, 79, 1084–1098.

Carpenter, M.A., Powell, R.A., and Salje, E.K.H. (1994) Thermodynamics of nonconvergent cation ordering in minerals: I. An alternative approach. American Mineralogist, 79, 1053–1067.

Gobbi, G.C., Christoffersen, R., Otten, M.T., Miner, B., Buseck, P.R., Kennedy, G.J., and Fyfe, C.A. (1985) Direct determination of cation disorder in $MgAl_2O_4$ spinel by high-resolution ^{27}Al magic-angle-spinning NMR spectroscopy. Chemistry Letters, 771–774.

Grimes, N.W. and Thompson, P. (1981) Space-group symmetry and structure parameter refinement for magnesium aluminate spinel. Acta Crystallographica, A37, C187.

Harrison, R.J. (1997) Magnetic properties of the magnetite-spinel solid solution. Ph.D. thesis, University of Cambridge.

Harrison, R.J. and Putnis, A. (1996) Magnetic properties of the magnetite-spinel solid solution: Curie temperatures, magnetic susceptibilities and cation ordering. American Mineralogist, 81, 375–384.

———(1997) The coupling between magnetic and cation ordering: A macroscopic approach. European Journal of Mineralogy, 9, 1115–1130.

Harrison, R.J., Redfern, S.A.T., and O'Neill, H.St.C. (1998a) The temperature dependence of the cation distribution in synthetic hercynite ($FeAl_2O_4$) from in-situ neutron structure refinements. American Mineralogist, 83, 1092–1099.

Harrison, R.J., Dove, M.T., Knight, K.S., and Putnis, A. (1998b) In situ neutron diffraction study of non-convergent ordering in the spinel solid solution $(Fe_3O_4)_{1-x}(MgAl_2O_4)_x$: kinetics and equilibrium ordering. American Mineralogist, in press.

Holland, T. and Powell, R. (1996) Thermodynamics of order-disorder in minerals: I. Symmetric formalism applied to minerals of fixed composition. American Mineralogist, 81, 1413–1424.

Hull, S., Smith, R.I., David, W.I.F., Hannon, A.C., Mayers, J., and Cywinski, R. (1992) The POLARIS powder diffractometer at ISIS. Physica B, 180, 1000–1002.

Hwang, L., Heuer, A.H., and Mitchell, T.E. (1973) On the space group of $MgAl_2O_4$ spinel. Philosophical Magazine, 28, 241–243.

Jorgensen, J.D., Faber, J., Carpenter, J.M., Crawford, R.K., Haumann, J.R., Hitterman, R.L., Kleb, R., Ostrowski, G.E., Rotella, F.J., and Worlton, T.G. (1989) Electronically focussed time-of-flight powder diffractometers at the intense pulsed neutron source. Journal of Applied Crystallography, 22, 321–333.

Klemme, S., O'Neill, H.St.C., and Green, D.H. (1997) The spinel-garnet lherzolite transition in the simple system CaO-MgO-Al_2O_3-SiO_2. The Australian National University, Research School of Earth Sciences, Annual Report, 1996, 87–88.

Landau, L.D. and Lifshitz, E.M. (1980) Statistical Physics, 544 p. Pergamon Press, Oxford, New York.

Larson, A.C. and Von Dreele, R.B. (1994) GSAS general structure analysis system. LANSCE MS-H805, Los Alamos National Laboratory.

Maekawa, H., Kato, S., Kawamura, K., and Yokokawa, T. (1997) Cation mixing in natural $MgAl_2O_4$ spinel: A high-temperature ^{27}Al NMR study. American Mineralogist, 82, 1125–1132.

Menegazzo, G., Carbonin, S., and Della Giusta, A. (1997) Cation and vacancy distribution in an artificially oxidised natural spinel. Mineralogical Magazine, 61, 411–421.

Millard, R.L., Peterson, R.C., and Hunter, B.K. (1992) Temperature dependence of cation disorder in $MgAl_2O_4$ spinel using ^{27}Al and ^{17}O magic-angle spinning NMR. American Mineralogist, 77, 44–52.

Mishra, R.K. and Thomas, G. (1977) Structural phase transition in the spinel $MgAl_2O_4$. Acta Crystallographica A33, 678–679.

Navrotsky, A. and Kleppa, O.J. (1967) The thermodynamics of cation distributions in simple spinels. Journal of Inorganic and Nuclear Chemistry, 29, 2701–2714.

Navrotsky, A., Wechsler, B.A., Geisinger, K., and Seifert, F. (1986) Thermochemistry of $MgAl_2O_4$-$Al_{8/3}O_4$ defect spinels. Journal of the American Chemical Society, 69, 418–422.

Nell, J., Wood, B.J., and Mason, T.O. (1989) High temperature cation distribution in Fe_3O_4-$MgFe_2O_4$-$FeAl_2O_4$-$MgAl_2O_4$ spinels from thermopower and conductivity measurements. American Mineralogist, 74, 339–351.

O'Neill, H.St.C. (1992) Temperature dependence of the cation distribution in zinc ferrite ($ZnFe_2O_4$) from powder XRD structural refinements. European Journal of Mineralogy, 4, 571–580.

———(1994) Temperature dependence of the cation distribution in $CoAl_2O_4$ spinel. European Journal of Mineralogy, 6, 603–609.

———(1997) Kinetics of the intersite cation exchange in $MgAl_2O_4$ spinel: the influence of nonstoichiometry. In Seventh Annual V.M. Goldschmidt Conference, p. 153. LPI Contribution No. 921, Lunar and Planetary Institute, Houston.

O'Neill, H.St.C. and Navrotsky, A. (1983) Simple spinels: crystallographic parameters, cation radii, lattice energies, and cation distribution. American Mineralogist, 68, 181–194.

———(1984) Cation distributions and thermodynamic properties of binary spinel solid solutions. American Mineralogist, 69, 733–753.

O'Neill, H.St.C., Annersten, H., and Virgo, D. (1992) The temperature dependence of the cation distribution in magnesioferrite ($MgFe_2O_4$) from powder XRD structural refinements and Mössbauer spectroscopy. American Mineralogist, 77, 725–740.

O'Neill, H.St.C., Dollase, W.A., and Ross, C.R. (1991) Temperature dependence of the cation distribution in nickel aluminate ($NiAl_2O_4$) spinel: a powder XRD study. Physics and Chemistry of Minerals, 18, 302–319.

Peterson, R.C., Lager, G.A., and Hitterman, R.L. (1991) A time-of-flight powder diffraction study of $MgAl_2O_4$ at temperatures up to 1273 K. American Mineralogist, 76, 1455–1458.

Redfern, S.A.T., Henderson, C.M.B., Wood, B.J., Harrison, R.J., and Knight, K.S. (1996) Determination of olivine cooling rates from metal-cation ordering. Nature, 381, 407–409.

Redfern, S.A.T., Henderson, C.M.B., Knight, K.S., and Wood, B.J. (1997) High-temperature order-disorder in $(Fe_{0.5}Mn_{0.5})_2SiO_4$ and $(Mg_{0.5}Mn_{0.5})_2SiO_4$ olivines: an in situ neutron diffraction study. European Journal of Mineralogy, 9, 287–300.

Salje, E.K.H. (1988) Kinetic rate laws as derived from order parameter theory I: Theoretical concepts. Physics and Chemistry of Minerals, 15, 336–348.

Schmocker, U. and Waldner, F. (1976) The inversion parameter with respect to the space group of $MgAl_2O_4$ spinels. Journal of Physic S: Solid State Physics, 9, L235–L237.

Smith, P.P.K. (1978) Note on the space group of spinel minerals. Philosophical Magazine, B38, 99–102.

Suzuki, I. and Kumazawa, M. (1980) Anomalous thermal expansion in spinel $MgAl_2O_4$, a possibility for a second order transition? Physics and Chemistry of Minerals, 5, 279–284.

Tokonami, M. and Horiuchi, H. (1980) On the space group of spinel, $MgAl_2O_4$. Acta Crystallographica, A36, 122–126.

Weeks, R.A. and Sonder, E. (1980) Electrical conductivity of pure and Fe-doped magnesium-aluminium spinel. Journal of the American Ceramic Society, 63, 92–95.

Wood, B.J., Kirkpatrick, R.J., and Montez, B. (1986) Order-disorder phenomena in $MgAl_2O_4$ spinel. American Mineralogist, 71, 999–1006.

Wu, C.C. and Mason, T.O. (1981) Thermopower measurement of cation distribution in magnetite. Journal of the American Ceramic Society, 64, 520–522.

Xu, H.W. and Heaney, P.J. (1997) Memory effects of domain structures during displacive phase transitions: A high-temperature TEM study of quartz and anorthite. American Mineralogist, 82, 99–108.

Yamanaka, T. and Takéuchi, Y. (1983) Order-disorder transition in $MgAl_2O_4$ spinel at high temperatures up to 1700 °C. Zeitshrift für Kristallographie, 165, 65–78.

Manuscript received July 8, 1998
Manuscript accepted September 19, 1998
Paper handled by Robert M. Hazen